Rapid Communications

Magnonic quantum spin Hall state in the zigzag and stripe phases of the antiferromagnetic honeycomb lattice

Ki Hoon Lee,[1,2,*] Suk Bum Chung,[1,2,3,†] Kisoo Park,[1,2] and Je-Geun Park[1,2]

[1]*Center for Correlated Electron Systems, Institute for Basic Science (IBS), Seoul National University, Seoul 08826, Korea*

[2]*Department of Physics and Astronomy, Seoul National University, Seoul 08826, Korea*

[3]*Department of Physics, University of Seoul, Seoul 02504, Korea*

(Received 28 December 2017; published 4 May 2018)

We investigated the topological property of magnon bands in the collinear magnetic orders of zigzag and stripe phases for the antiferromagnetic honeycomb lattice and identified Berry curvature and symmetry constraints on the magnon band structure. Different symmetries of both zigzag and stripe phases lead to different topological properties, in particular, the magnon bands of the stripe phase being disentangled with a finite Dzyaloshinskii-Moriya (DM) term with nonzero spin Chern number. This is corroborated by calculating the spin Nernst effect. Our study establishes the existence of a nontrivial magnon band topology for all observed collinear antiferromagnetic honeycomb lattices in the presence of the DM term.

DOI: 10.1103/PhysRevB.97.180401

Introduction. Over the past few decades, topology has emerged as a long-ignored yet most revolutionary concept in condensed matter physics [1]. In particular, the last few years have witnessed an intensive worldwide search for topological phases in electronic systems [2–6]. More recently, another race began in the search for analogous phases in bosonic systems, with a few notable examples already given: gapped spin liquids, photonic band-gap materials, and magnon insulators [7–14]. The realization that the Bloch theorem holds for both bosonic and electronic band structures has also led to a couple of new topological magnon bands, in pyrochlore lattices [15–19] and in two-dimensional (2D) kagome lattices [20,21]. In light of the recent experimental realization of monolayer magnetic honeycomb lattices of $NiPS_3$ and $FePS_3$ [22,23], $Cr_2Ge_2Te_6$ [24], and CrI_3 [25], the topological character of the magnon band in a honeycomb lattice is not only of theoretical interest but also of experimental relevance.

Previous studies of magnon band topology for the honeycomb lattice were restricted to the ferromagnetic and Néel phases. It has been shown that the former exhibits a magnon band structure with Dirac points occurring at each valley point [26,27], which is gapped out by the next-nearest-neighbor Dzyaloshinskii-Moriya (DM) interaction producing a magnon analog of the quantum anomalous Hall (QAH) phase [28,29]. However, a finite DM interaction added to the latter phase, while giving rise to the spin Nernst effect, does not yield a topological magnon band structure [30,31]. In addition, for the S_z conserving phases, another possible topological phase is a magnon analog of the quantum spin Hall (QSH) phase arising from a well-defined spin Chern number [32]. To the best of our knowledge, a simple model for this topological phase is lacking; the models proposed so far for a magnon analog of the QSH include either a bilayer honeycomb with antiferromagnetic interlayer coupling [30,33] or a dipolar interaction [34] with the Aharonov-Casher effect on magnon bands under an external electric field for a square lattice [35]. This motivates us to study the magnon topology of other physically feasible collinear spin ordered phases in the honeycomb spin Hamiltonian, the zigzag and stripe phases.

In this Rapid Communication, we examine the topological properties of these two phases on a monolayer honeycomb lattice. Our study finds that for both phases the nontrivial Berry phase and Dirac magnon point are protected by spatial (glide) mirror symmetry. We show that with the DM interaction, the stripe phase hosts a magnon analog of the QSH phase. We demonstrate that the resulting band topology is that of a $\mathcal{C}_S = 1$ QSH, not a $\mathcal{C} = 1$ QAH, by computing its spin Berry curvature and edge states for a finite width lattice. By contrast, we find that the zigzag phase has a nodal line protected by nonsymmorphic symmetry combined with time-reversal symmetry. For both phases, we also calculate the spin Nernst effect, which is the manifestation of nontrivial topology and a direct consequence of nontrivial magnon Berry curvature. In the remainder of this Rapid Communication, we will first explain our spin model for a monolayer honeycomb lattice and the method we used to calculate the magnon band, before presenting our results for the zigzag and stripe phases.

Model. We consider a J_1-J_2-J_3 model for a honeycomb lattice with a next-nearest-neighbor DMI,

$$H_0 = \sum_{n=1}^{3} J_n \sum_{\langle i,j\rangle_n} \boldsymbol{S}_i \cdot \boldsymbol{S}_j + J_{\mathrm{DM}} \sum_{\langle i,j\rangle_2} \nu_{ij} \hat{\boldsymbol{z}} \cdot (\boldsymbol{S}_i \times \boldsymbol{S}_j), \quad (1)$$

where $\boldsymbol{S}_i$ is spin at site i with size S and $\langle i,j\rangle_n$ is a pair of nth nearest neighbors, $\nu_{ij} = \mathrm{sgn} \sum_{\langle i,k\rangle_1, \langle k,j\rangle_1} \hat{\boldsymbol{z}} \cdot \boldsymbol{r}_{ik} \times \boldsymbol{r}_{kj}$, where $\boldsymbol{r}_{ij} = \boldsymbol{r}_i - \boldsymbol{r}_j$ and $\boldsymbol{r}_i$ is the coordinate of the ith site. Note that there is only one k simultaneously satisfying both conditions $\langle i,k\rangle_1$ and $\langle k,j\rangle_1$ for a given second-nearest-neighbor pair $\langle i,j\rangle_2$. While our analysis is intended to be of general applicability, the Hamiltonian is mostly relevant to the single-layer

*kihoonlee@snu.ac.kr

†sbchung0@uos.ac.kr

van der Waals magnetic material family MAX_3, such as $NiPS_3$ and $FePS_3$ [22,23,36]. In the phase diagram of J_1, J_2, and J_3, several ground states were identified, such as ferromagnetic (FM), Néel, zigzag, and stripe phases, while other noncollinear phases can also appear for both cases of $J_1 > 0$ and $J_1 < 0$ [37]; for instance, the zigzag phase for $J_1 > 0$ appears within $J_2/J_1, J_3/J_1 > 0.5$, and we will examine the stripe phase later in this Rapid Communication. While these phases are not very common, there are materials such as $BaNi_2As_2O_8$ showing zigzag order arising from the J_1-J_2-J_3 model [38].

It is important to note that spin-orbit coupling, if not zero, has a crucial consequence on the symmetry of the magnetic Hamiltonian and its ground state. For nonzero spin-orbit coupling, the symmetric point group of the magnon Hamiltonian for the magnetic ground state contains operations acting both on the spin and lattice. But if the spin-orbit coupling is small enough, we can ignore some of the anisotropic exchange or higher-order single-ion anisotropy. Such an assumption allows us to reduce the Hamiltonian to have a symmetry higher than the (magnetic) space group, and such a symmetry group is called a spin-space group [39]. For example, a ferromagnetic magnon band structure in a honeycomb has crossings at the K points if only Heisenberg terms exist in the spin Hamiltonian [26]. But once the lattice symmetry-allowed DMI, which requires the spin-orbit coupling (SOC) to have a nonzero value, is introduced, the gap is opened [29]. While both Hamiltonians are allowed by the lattice symmetry, the spin-space group of the first case without DMI has a higher symmetry that protects the crossings at the K points.

Method. We study the magnon bands of the zigzag and stripe phases using the linear spin-wave theory (LSWT). We take the z direction to be the easy axis, which is relevant to the anisotropic DM interaction. Applying a Holstein-Primarkoff (HP) transformation to spin $\tilde{\boldsymbol{S}}_i$ in the local spin coordinates by taking the local magnetization direction as the z direction and $\tilde{S}^+ \simeq \sqrt{2S}a$, $\tilde{S}^- \simeq \sqrt{2S}a^\dagger$, $\tilde{S}_z = S - a^\dagger a$, we obtain a quadratic HP boson Hamiltonian in the following form,

$$H = \frac{1}{2}\sum_{\alpha,\beta,\boldsymbol{k}} \psi^\dagger_{\alpha\boldsymbol{k}} H_{\alpha\beta}(\boldsymbol{k})\psi_{\beta\boldsymbol{k}}$$
$$= \frac{1}{2}\sum_{\boldsymbol{k},\eta}[E_\eta(\boldsymbol{k})\gamma^\dagger_{\eta\boldsymbol{k}}\gamma_{\eta\boldsymbol{k}} + E_\eta(-\boldsymbol{k})\gamma_{\eta,-\boldsymbol{k}}\gamma^\dagger_{\eta,-\boldsymbol{k}}], \quad (2)$$

where $\psi_{\alpha\boldsymbol{k}} = (a_{\alpha,\boldsymbol{k}}, a^\dagger_{\alpha,-\boldsymbol{k}})^T$ is the Nambu spinor of the HP boson, α,β are sublattice indices, and η is the band index. The Hamiltonian can be diagonalized by a paraunitary matrix $T(\boldsymbol{k})$ satisfying $\sum_\eta(\gamma^\dagger_{\eta\boldsymbol{k}}, \gamma_{\eta,-\boldsymbol{k}})T^\dagger_{\eta\alpha}(\boldsymbol{k}) = \psi^\dagger_{\alpha\boldsymbol{k}}$, $\sigma_3 = T^\dagger(\boldsymbol{k})\sigma_3 T(\boldsymbol{k}) = T(\boldsymbol{k})\sigma_3 T^\dagger(\boldsymbol{k})$, and $\sum_{\alpha,\beta} T^\dagger_{\eta\alpha}(\boldsymbol{k})H_{\alpha\beta}(\boldsymbol{k})T_{\beta\eta'}(\boldsymbol{k}) = \delta_{\eta\eta'}\,\mathrm{diag}\{E_\eta(\boldsymbol{k}), E_\eta(-\boldsymbol{k})\}$, where σ_3 is the Pauli matrix operator acting on particle-hole space [40,41]; for explicit forms of the Hamiltonians, see the Supplemental Material [42].

Zigzag phase. In analyzing the magnon band structure for the zigzag phase, its symmetry properties need to be considered. First, we note that the zigzag phase has a doubled unit cell consisting of four lattice sites and a spin configuration as shown in the inset of Fig. 1(a). Second, the symmetry group of Eq. (2) is composed of elements of the space group

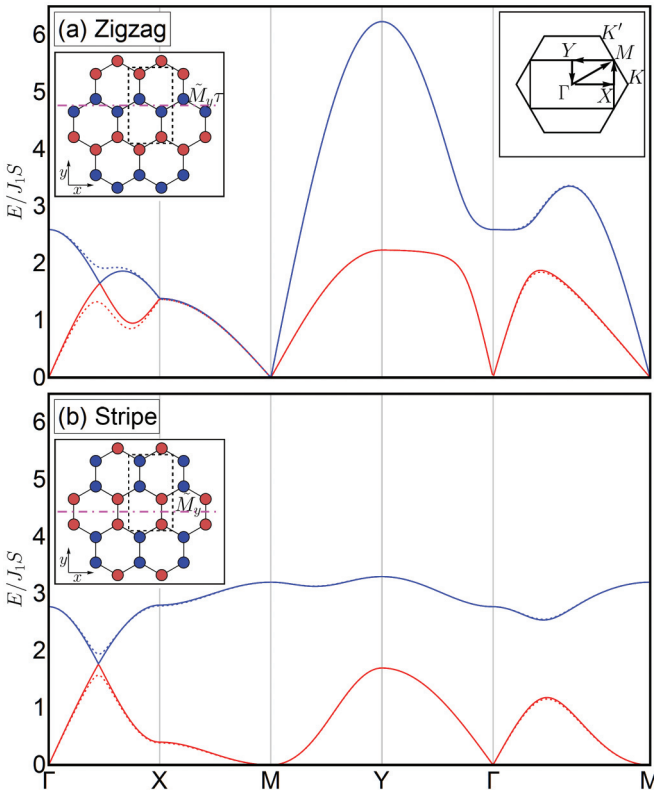

FIG. 1. Magnon band structure for each phase following the paths in the inset of (a). The solid (dashed) line is without (with) DMI. The figures in the insets represent the ground-state configurations, and each color represents opposite s_z components. We can find a Dirac magnon on the Γ-X line, which can be gapped by DMI. The zigzag phase has fourfold degeneracy on the X-M line, which is protected by nonsymmorphic symmetry combined with time-reversal symmetry. We used the following parameters for the zigzag phase ($J_2 = 0.8J_1$, $J_3 = 0.8J_1$) and for the stripe phase ($J_2 = 0.4J_1$, $J_3 = -0.2J_1$).

of Eq. (1) that does not alter the magnetic ground state. The universal symmetry of a collinear phase is C_∞ of spin, which is a subgroup of the SO(3) of Eq. (1) and generated by S_z. Therefore, combining with translation symmetry, we can assign two eigenvalues to an energy eigenstate, a magnetic moment along the magnetization axis s_z, and crystal momentum $\boldsymbol{k}$ in the magnetic Brillouin zone (MBZ). In the presence of an additional symmetry operator A that commutes with translation, we will consider two specific cases. The first case is where the two operators commute, for which we can simply add another eigenvalue to label an energy eigenstate. The second case is where two operators anticommute and it guarantees twofold degeneracy. To show this, let us assume an energy eigenstate $|s_z,\boldsymbol{k}\rangle$ labeled by s_z and $\boldsymbol{k}$. The anticommutation $\{S_z, A\} = 0$ guarantees that A should flip the sign of s_z, i.e., $S_z(A|s_z,\boldsymbol{k}\rangle) = -AS_z|s_z,\boldsymbol{k}\rangle = -s_z(A|s_z,\boldsymbol{k}\rangle)$, from which we obtain the twofold degeneracy through $H|-s_z,\boldsymbol{k}\rangle = HA|s_z,\boldsymbol{k}\rangle = AH|s_z,\boldsymbol{k}\rangle = EA|s_z,\boldsymbol{k}\rangle = E|-s_z,\boldsymbol{k}\rangle$ (note that if $s_z \neq 0$, $A|s_z,\boldsymbol{k}\rangle \neq |s_z,\boldsymbol{k}\rangle$).

In a collinear AFM phase, there are various symmetry operators that combine exchanging sublattices with flipping spins either through twofold spin rotation or time reversal. One such symmetry that does not affect crystal momentum is

$C_{2z}\Theta$, where Θ is the time-reversal operation. We have $C_{2z}\Theta$ symmetry all in the zigzag, stripe, and Néel phases of the honeycomb lattice. Twofold rotation is located at the center of the honeycomb for the zigzag and Néel phases whereas it is at the center of a bonding connecting sites with opposite spin configuration for the stripe phase. We show below that the two relevant symmetries of the zigzag phase that commute with S_z are the glide mirror $\tilde{M}_y\tau_x$, where τ_x is the half unit cell lattice translation in the x direction (defined in Fig. 1), and $\tilde{M}_y e^{i\pi S_x}\tau_x\Theta$; the symmetry operators with the tilde sign here act only on the lattice.

$\tilde{M}_y\tau_x$ protects the two accidental band crossings on the mirror-symmetric line $k_y = 0$ for $J_{\rm DM} = 0$, at which it commutes with the Hamiltonian of Eq. (1) [43]. However, for $J_{\rm DM} \neq 0$ as in the Néel phase, it removes this accidental degeneracy as it breaks $\tilde{M}_y\tau_x$ symmetry due to the pseudoscalar $\nu_{ij} \equiv \mathrm{sgn}\sum_{\langle i,k\rangle_1,\langle k,j\rangle_1} \hat{\boldsymbol{z}}\cdot(\boldsymbol{r}_{ik}\times\boldsymbol{r}_{kj})$ reversing sign under the mirror operation $\tilde{M}_y$. The eigenvalues of the glide mirror $\tilde{M}_y\tau_x$ are $\pm e^{ik_x/2}$ due to $(\tilde{M}_y\tau_x)^2 = \tau_x^2$, and for $J_{\rm DM} = 0$ we can simply assign the same glide mirror eigenvalue to a pair of degenerate bands with an opposite S_z eigenvalue as $\tilde{M}_y\tau_x$ commutes with S_z. The protection for the accidental crossing between two doubly degenerate bands at $J_{\rm DM} = 0$ requires their glide mirror eigenvalues to be opposite. That is exactly the case we found in our work for the zigzag phase, because there is no diagonal term in the representation of $\tilde{M}_y\tau_x$. The sum of mirror eigenvalues of all bands vanishes as $\tilde{M}_y\tau_x$ changes the position of every sublattice. While glide mirror symmetry protects the existing accidental crossings, it does not necessarily guarantee their existence. For an accidental crossing to exist on the Γ-X symmetric line, we need to have $[E_+(\Gamma) - E_-(\Gamma)][\partial_{k_x}E_+(X) - \partial_{k_x}E_-(X)] < 0$, where $E_\pm$ is the dispersion of bands with $\pm e^{ik_x/2}$ glide mirror eigenvalues. This condition arises out of the constraint $E_+(X) = E_-(X)$, which is required by the symmetry that we will now discuss.

At the zone boundary, a glide mirror combined with time-reversal symmetry $g = M_y\tau_x\Theta = \tilde{M}_y e^{i\pi S_x}\tau_x\Theta$ produces the constraint that two bands with opposite glide mirror eigenvalues should be degenerate [43] as long as the zigzag phase is stable. Not only is g a symmetry, but we have $g^2 = -1$ at the MBZ boundary $k_x = \pi$ as $\tau_x^2 = e^{ik_x} = -1$ holds there. An antiunitary symmetry whose square is -1 gives a Kramer-type degeneracy, and—as the operator commutes with S_z—altogether, fourfold degeneracy arises, which leads to the sticking of all bands at the zone boundary. Therefore, at the zone boundary $k_x = \pi$, all four bands are degenerate and so cannot be split [44]. It holds even in the presence of the DM interaction as it does not break the symmetry g.

Stripe phase. The stripe phase has a unit cell identical to that of the zigzag phase with the spin configurations shown in the inset of Fig. 1(b). The stripe phase has twofold degeneracy because of the degeneracy between states with opposite s_z as in the zigzag phase. If $J_{\rm DM} = 0$, the stripe phase has a spatial mirror symmetry $\tilde{M}_y$, which protects the accidental crossing on the mirror invariant line $k_y = 0$ for the same reason that the glide mirror symmetry protects that of the zigzag phase. The condition to have crossing is $[E_+(\Gamma) - E_-(\Gamma)][E_+(X) - E_-(X)] < 0$, where $E_\pm(\boldsymbol{k})$ is the dispersion of the band with a $\pm$ mirror eigenvalue at a given momentum $\boldsymbol{k}$.

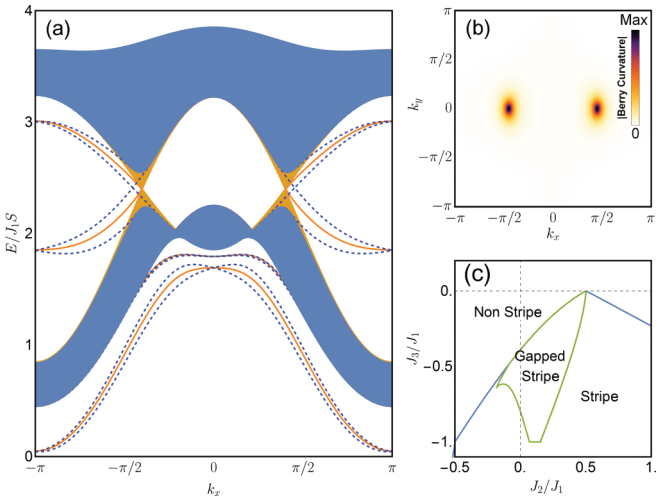

FIG. 2. (a) Band structure for the stripe phase with finite width along the zigzag direction of a honeycomb lattice with DMI (blue) or without DMI (yellow). Lines are the edge states calculated from a finite width of 40 magnetic unit cells and the colored region represents the bulk bands. To remove the instability from near the edge, we added an easy-axis anisotropy term $0.3J_1(1 - S_z^2)$. Other parameters are kept the same as in Fig. 1. To find at which side the edge modes are localized, see the Supplemental Material [42]. (b) Berry curvature in the Brillouin zone. (c) Gapped stripe phase on top of classical phase diagram of J_1-J_2-J_3 for $J_1 > 0$ (the zigzag phase would require a larger positive J_3/J_1).

With the DM interaction, the stripe phase can exhibit a magnon band structure that is both insulatorlike and topologically nontrivial. This is because the DM interaction breaks the spatial mirror symmetry $\tilde{M}_y$ and opens the band crossing as in the zigzag phase. As this occurs without any nonsymmorphic symmetry constraining bands to be degenerate, two bands can be split to make the magnon band structure insulatorlike, as depicted in Fig. 1(b) with a proper choice of parameters. In such a case, the topology of the lower band is well defined, with the topological invariant under S_z conservation being the spin Chern number. The Berry curvature of the nth band is defined as $\Omega_n(\boldsymbol{k}) = i\epsilon_{\mu\nu z}[\sigma_3\partial_{k_\mu}T_{\boldsymbol{k}}^\dagger\sigma_3\partial_{k_\nu}T_{\boldsymbol{k}}]_{nn}$ [45,46]. In general, a degenerate band will not have a well-defined Berry curvature on its own, but we can separate a pair of degenerate bands using S_z conservation. The Berry curvature of a band with a well-defined S_z eigenvalue is shown in Fig. 2(b), and we note that the Berry curvature is concentrated near the band edge. The Chern number can be defined for each band as $\mathcal{C}_n = \frac{1}{2\pi}\int dk_x dk_y \Omega_n(\boldsymbol{k})$. The spin Chern number of doubly degenerated lower bands is $\mathcal{C}_S = (\mathcal{C}_\uparrow - \mathcal{C}_\downarrow)/2$, where $\mathcal{C}_\uparrow$ ($\mathcal{C}_\downarrow$) is the Chern number of $s_z = 1$ ($s_z = -1$) [30,47]. The Chern number for each is an integer and opposite in sign (i.e., $\mathcal{C}_\uparrow = -\mathcal{C}_\downarrow$), because two bands are related by an antiunitary operator $C_{2z}\Theta$. Therefore, $\mathcal{C}_S$ is also quantized to be an integer and for the stripe phase $\mathcal{C}_S = \mathrm{sgn}(J_{\rm DM})$. In this sense, the band topology is analogous to that of the QSH insulator discussed in Ref. [32].

It is important to comment that the nontrivial topological number of bosonic bands cannot give rise to a quantized transverse response as in fermionic systems. It is because

a bosonic band, lacking the Pauli exclusion principle, cannot be filled uniformly, the only possible exception being the low-temperature transverse conductivity divided by the temperature-dependent bosonic occupation number where the lowest band is flat and well separated from other bands [35]. While a nontrivial bosonic band topology can give rise to edge states, their spectra need to lie within the bulk energy gap in order for them to make a greater contribution to the transport properties. The stripe phase can stabilize such a gapped magnon band structure over a finite parameter space at $J_{\rm DM}/J_1 = 0.05$, as shown in Fig. 2(c). In this case, we can have an effective edge magnon transport, as the decay of edge modes to the bulk states requires inelastic scattering due to the edge modes being inside the bulk band gap; recently, it has been reported that such edge transport is more robust against disorder than bulk transport [48].

The dispersion of edge states between the lower and upper bands of the stripe phase is shown in Fig. 2(a). The edge modes carry the S_z spin as the HP boson Hamiltonian still commutes with S_z in the nanoribbon geometry. There are two types of terminations possible, and each type determines the center position of the edge modes (whether it is to appear in $-\pi > k_x > 0$ or $0 < k_x < \pi$). We also had to include a term for easy-axis anisotropy for the nanoribbon geometry calculations to prevent an exponentially decaying deviation from appearing near the edges of the stripe configuration. This instability is naturally expected as the coordination number is reduced near the edges. We comment that small noncollinearity will introduce a small gap on the edge modes.

Although the spin Berry curvature does not give quantized responses, we still can obtain a finite transverse response. For example, the FM phase shows a finite thermal Hall effect due to magnons. Similarly, for the Néel phase, the spin Nernst effect (SNE) was obtained for a finite DM interaction [30,31]. The SNE is given by the thermal spin Hall conductivity $\alpha^s_{xy} = -\frac{1}{T}\sum_{kn}(S_z\sigma_3)_{nn}\Omega_n(\boldsymbol{k})\int_0^{E_n(\boldsymbol{k})} d\eta\eta\frac{dg(\eta)}{d\eta}$, where $g(\eta)$ is the Bose-Einstein distribution function, n is the band index, and the band index summation is limited to a particle band [30]. The thermal spin Hall conductivity calculated for both zigzag and stripe phases is shown in Fig. 3. We find a sign change of SNE in the zigzag phase, which can also be found in the Néel phase [31]. It is due to the Berry curvature sign not being constant over the MBZ in the zigzag phase [42].

In passing, we would like to comment that both zigzag and stripe phases also appear in extended Kitaev Hamiltonians [49–53], but the staggered moment is not out of plane, and the Kitaev and Γ terms break SO(2) symmetry. As a result, neither the spin carried by magnons nor the spin Chern number relying on S_z conservation are well defined.

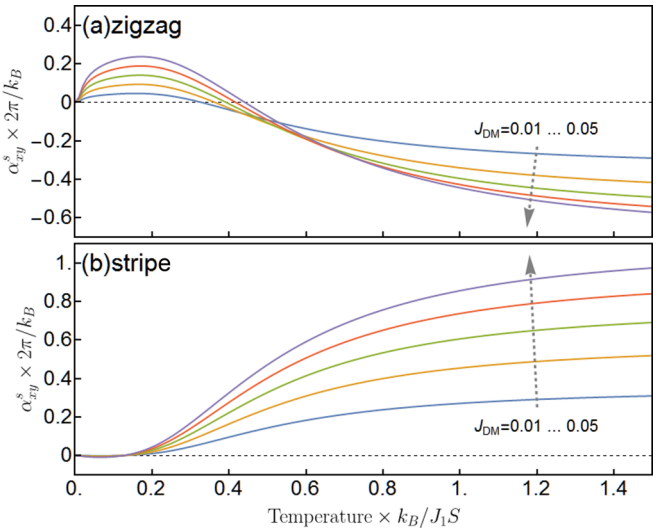

FIG. 3. Spin Nernst effect in the (a) zigzag phase and (b) stripe phase with varying $J_{\rm DM}$.

Conclusions. We have studied the magnon band structure of zigzag and stripe phases for the J_1-J_2-J_3 Heisenberg model with and without DMI for a honeycomb lattice. In both phases, we found a Dirac magnon, where the accidental crossing is protected by spatial glide mirror or mirror symmetry and the gap can be opened by the DM interaction, but with different topological phases for different symmetries. For the zigzag phase, which is commonly found in magnetic systems with a honeycomb lattice, we found that a nonsymmorphic symmetry combined with time reversal gives rise to a topologically protected line node at the zone boundary. On the other hand, for the stripe phase, we found that it is possible to realize the magnon analog of QSH.

Note added. Recently, we became aware of a related paper [54], which has obtained a similar result for the zigzag and stripe phases for a Hamiltonian without DMI.

Acknowledgments. We thank SungBin Lee, Cheol-Hwan Park, and Bohm Jung Yang for their useful comments. The work at the IBS CCES was supported by the Institute for Basic Science in Korea (IBS-R009-G1, IBS-R009-Y1, and IBS-R009-D1).

[1] F. D. M. Haldane, Rev. Mod. Phys. **89**, 040502 (2017).
[2] M. Z. Hasan and C. L. Kane, Rev. Mod. Phys. **82**, 3045 (2010).
[3] X.-L. Qi and S.-C. Zhang, Rev. Mod. Phys. **83**, 1057 (2011).
[4] Y. Ando, J. Phys. Soc. Jpn. **82**, 102001 (2013).
[5] B. A. Bernevig and T. L. Hughes, *Topological Insulators and Topological Superconductors* (Princeton University Press, Princeton, NJ, 2013).
[6] C.-K. Chiu, J. C. Teo, A. P. Schnyder, and S. Ryu, Rev. Mod. Phys. **88**, 035005 (2016).
[7] V. Kalmeyer and R. B. Laughlin, Phys. Rev. Lett. **59**, 2095 (1987).
[8] A. Kitaev, Ann. Phys. **321**, 2 (2006).
[9] A. Banerjee, C. A. Bridges, J. Q. Yan, A. A. Aczel, L. Li, M. B. Stone, G. E. Granroth, M. D. Lumsden, Y. Yiu, J. Knolle, S. Bhattacharjee, D. L. Kovrizhin, R. Moessner, D. A. Tennant, D. G. Mandrus, and S. E. Nagler, Nat. Mater. **15**, 733 (2016).
[10] S.-H. Do, S.-Y. Park, J. Yoshitake, J. Nasu, Y. Motome, Y. S. Kwon, D. T. Adroja, D. J. Voneshen, K. Kim, T. H. Jang, J. H. Park, K.-Y. Choi, and S. Ji, Nat. Phys. **13**, 1079 (2017).

[11] F. D. M. Haldane and S. Raghu, Phys. Rev. Lett. **100**, 013904 (2008).

[12] Z. Wang, Y. D. Chong, J. D. Joannopoulos, and M. Soljačić, Phys. Rev. Lett. **100**, 013905 (2008).

[13] Z. Wang, Y. Chong, J. D. Joannopoulos, and M. Soljačić, Nature (London) **461**, 772 (2009).

[14] L. Zhang, J. Ren, J.-S. Wang, and B. Li, Phys. Rev. B **87**, 144101 (2013).

[15] A. Mook, J. Henk, and I. Mertig, Phys. Rev. Lett. **117**, 157204 (2016).

[16] F.-Y. Li, Y.-D. Li, Y. B. Kim, L. Balents, Y. Yu, and G. Chen, Nat. Commun. **7**, 12691 (2016).

[17] A. Mook, J. Henk, and I. Mertig, Phys. Rev. B **95**, 014418 (2017).

[18] Y. Su, Phys. Rev. B **95**, 224403 (2017).

[19] S.-K. Jian and W. Nie, Phys. Rev. B **97**, 115162 (2018).

[20] A. Mook, J. Henk, and I. Mertig, Phys. Rev. B **89**, 134409 (2014).

[21] R. Chisnell, J. S. Helton, D. E. Freedman, D. K. Singh, R. I. Bewley, D. G. Nocera, and Y. S. Lee, Phys. Rev. Lett. **115**, 147201 (2015).

[22] C.-T. Kuo, M. Neumann, K. Balamurugan, H. J. Park, S. Kang, H. W. Shiu, J. H. Kang, B. H. Hong, M. Han, T. W. Noh *et al.*, Sci. Rep. **6**, 20904 (2016).

[23] J.-U. Lee, S. Lee, J. H. Ryoo, S. Kang, T. Y. Kim, P. Kim, C.-H. Park, J.-G. Park, and H. Cheong, Nano Lett. **16**, 7433 (2016).

[24] C. Gong, L. Li, Z. Li, H. Ji, A. Stern, Y. Xia, T. Cao, W. Bao, C. Wang, Y. Wang, Z. Q. Qiu, R. J. Cava, S. G. Louie, J. Xia, and X. Zhang, Nature (London) **546**, 265 (2017).

[25] B. Huang, G. Clark, E. Navarro-Moratalla, D. R. Klein, R. Cheng, K. L. Seyler, D. Zhong, E. Schmidgall, M. A. McGuire, D. H. Cobden *et al.*, Nature (London) **546**, 270 (2017).

[26] J. Fransson, A. M. Black-Schaffer, and A. V. Balatsky, Phys. Rev. B **94**, 075401 (2016).

[27] S. S. Pershoguba, S. Banerjee, J. C. Lashley, J. Park, H. Agren, G. Aeppli, and A. V. Balatsky, Phys. Rev. X **8**, 011010 (2018).

[28] S. K. Kim, H. Ochoa, R. Zarzuela, and Y. Tserkovnyak, Phys. Rev. Lett. **117**, 227201 (2016).

[29] S. A. Owerre, J. Phys.: Condens. Matter **28**, 386001 (2016).

[30] V. A. Zyuzin and A. A. Kovalev, Phys. Rev. Lett. **117**, 217203 (2016).

[31] R. Cheng, S. Okamoto, and D. Xiao, Phys. Rev. Lett. **117**, 217202 (2016).

[32] Y. Yang, Z. Xu, L. Sheng, B. Wang, D. Y. Xing, and D. N. Sheng, Phys. Rev. Lett. **107**, 066602 (2011).

[33] S. A. Owerre, Phys. Rev. B **94**, 094405 (2016).

[34] X. S. Wang and X. R. Wang, J. Phys. D: Appl. Phys. **51**, 194001 (2018).

[35] K. Nakata, J. Klinovaja, and D. Loss, Phys. Rev. B **95**, 125429 (2017).

[36] J.-G. Park, J. Phys.: Condens. Matter **28**, 301001 (2016).

[37] J. B. Fouet, P. Sindzingre, and C. Lhuillier, Eur. Phys. J. B **20**, 241 (2001).

[38] L. Regnault, J. Henry, J. Rossat-Mignod, and A. De Combarieu, J. Magn. Magn. Mater. **15**, 1021 (1980).

[39] W. F. Brinkman and R. J. Elliott, Proc. R. Soc. London, Ser. A **294**, 343 (1966).

[40] J. H. P. Colpa, Physica A **93**, 327 (1978).

[41] R. Shindou, R. Matsumoto, S. Murakami, and J.-i. Ohe, Phys. Rev. B **87**, 174427 (2013).

[42] See Supplemental Material at http://link.aps.org/supplemental/10.1103/PhysRevB.97.180401 for the representation of the HP boson Hamiltonians, the Berry curvature in the zigzag phase and the detail of edge states in the stripe phase.

[43] S. M. Young and C. L. Kane, Phys. Rev. Lett. **115**, 126803 (2015).

[44] S. A. Parameswaran, A. M. Turner, D. P. Arovas, and A. Vishwanath, Nat. Phys. **9**, 2600 (2013).

[45] R. Matsumoto, R. Shindou, and S. Murakami, Phys. Rev. B **89**, 054420 (2014).

[46] S. Murakami and A. Okamoto, J. Phys. Soc. Jpn. **86**, 011010 (2016).

[47] K. Nakata, S. K. Kim, J. Klinovaja, and D. Loss, Phys. Rev. B **96**, 224414 (2017).

[48] A. Rückriegel, A. Brataas, and R. A. Duine, Phys. Rev. B **97**, 081106 (2018).

[49] J. Chaloupka, G. Jackeli, and G. Khaliullin, Phys. Rev. Lett. **105**, 027204 (2010).

[50] J. Chaloupka, G. Jackeli, and G. Khaliullin, Phys. Rev. Lett. **110**, 097204 (2013).

[51] J. G. Rau, E. K.-H. Lee, and H. Y. Kee, Phys. Rev. Lett. **112**, 077204 (2014).

[52] Y. Singh, S. Manni, J. Reuther, T. Berlijn, R. Thomale, W. Ku, S. Trebst, and P. Gegenwart, Phys. Rev. Lett. **108**, 127203 (2012).

[53] X. Liu, T. Berlijn, W.-G. Yin, W. Ku, A. Tsvelik, Y.-J. Kim, H. Gretarsson, Y. Singh, P. Gegenwart, and J. P. Hill, Phys. Rev. B **83**, 220403 (2011).

[54] D. Boyko, J. T. Haraldsen, and A. V. Balatsky, Phys. Rev. B **97**, 014433 (2018).